Int J Thermophys (2008) 29:370–385
DOI 10.1007/s10765-007-0323-7

# Spectral and Total Effective Emissivity of a High-Temperature Fixed-Point Radiator Considered in Relation to the Temperature Drop Across its Back Wall

**P. Bloembergen · B. B. Khlevnoy · P. Jimeno Largo · Y. Yamada**

Published online: 5 February 2008


**Abstract** In this article, calculations of the spectral and total cavity emissivity of a high-temperature fixed-point radiator by means of the Monte–Carlo technique in conjunction with calculations of the temperature drop across its back wall using the finite-element approach are presented. The temperature drop across the back wall of a fixed-point cavity radiator is influenced by the heat exchange within the cavity and between the cavity and the front end of the associated furnace. The special effects of these influences were virtually neglected in earlier estimates of the temperature drop for high-temperature fixed-point radiators, resulting in an overestimation of the value of this parameter. These same effects have a non-negligible influence on the cavity emissivity. Even though the heat exchange between the furnace and cavity enhances the temperature uniformity within the cavity, it appears that the cavity cannot be assumed to be isothermal for the case considered, as is usually taken for granted when dealing with fixed-point cavity radiators. Since the temperature drop and total emissivity are affected by the same thermophysical processes, there exists a correlation between these parameters, which might find practical application. To provide experimental evidence to the findings inferred from the calculations, results of measurements of the

P. Bloembergen · Y. Yamada
National Metrology Institute of Japan, AIST,
1-1-1 Umezono, Tsukuba, Ibaraki 305-8563, Japan

P. Bloembergen (✉)
Zoeterwoudsesingel 78, Leiden, 2313 EL, The Netherlands
e-mail: p.bloembergen@aist.go.jp

B. B. Khlevnoy
All Russian Research Institute for Optical and Physical Measurements (VNIIOFI),
Moscow, Russia

P. Jimeno Largo
University of Valladolid, Valladolid, Spain

cavity radiance-temperature of two high-temperature fixed-point cells are presented, enclosing an ingot of eutectic Re-C, for which the cavities are provided with different apertures. For $\lambda = 650\,\text{nm}$, the measured differences in cavity radiance-temperature are shown to be compatible with the differences in radiance temperature calculated for these cavities.

**Keywords** Emissivity · Fixed points · High temperatures · Reflectivity · Temperature drop

## 1 Introduction

At high temperatures, the temperature drop $\Delta T$ across the back wall of a fixed-point cavity radiator and the cavity's spectral and total emissivity are influenced by the heat exchange within the cavity and between the cavity and the front end of the associated furnace, precluding treating the cavity as a separate unit. In this article, these influences are evaluated by varying the cavity-aperture diameter and furnace-temperature profile.

At or below the copper point, the correction for the temperature drop has been found to be smaller than the uncertainty in the fixed-point realization itself. Since radiative heat exchange increases with $T^4$, the situation is quite different for high-temperature fixed-points such as the metal-carbon or metal carbide–carbon eutectic fixed-points [1], to the extent that the uncertainty in the temperature drop may be one of the dominant components in the overall uncertainty.

This study (a) is to be considered a follow-up to [2] which established the *temperature drop* $\Delta T = T_{\text{FP}} - T_{\text{cav}}$ across the back wall of a high-temperature fixed-point radiator by means of finite-element analysis and (b) extends what was already concisely presented in [3] and [4]. Here we concentrate on quantifying the *cavity emissivity* needed to determine the *cavity* temperature $T_{\text{cav}}$ and thus to obtain the fixed-point temperature $T_{\text{FP}} = T_{\text{cav}} + \Delta T$ of the system in question.

As in [2], the example chosen (Sect. 2) is a cavity with specified dimensions surrounded by an ingot of eutectic Re-C, radiating at the eutectic temperature $T_{\text{FP}} = T_{\text{E}}$ of 2,748 K. The temperature drop $\Delta T$ is modeled by means of finite-element calculus, whereas the spectral and total cavity emissivities are calculated independently by the Monte–Carlo technique (Sect. 3).

Results of calculations of spectral and total emissivities are discussed in relation to the temperature drop $\Delta T$ and the cavity-temperature profile which, even though it concerns a fixed-point cavity, is shown to be non-isothermal (Sect. 4.1). By comparison with results calculated for an isothermal cavity, the non-uniformity of the cavity temperature is shown to have a non-negligible influence on both the spectral and total emissivity. On the other hand, we will show that the differences in emissivities calculated for the non-isothermal cavity and the isothermal cavity, although significant, do not depend strongly on the furnace-temperature profile, which might be of practical interest (Sect. 4.2).

An obvious issue is to track the temperature drop in relation to the total emissivity, noticing that both parameters are intimately connected with the total radiative flux emitted by the cavity. Within a certain uncertainty band, a linear correlation between

temperature drop $\Delta T$ and total reflectivity, calculated for both the non-isothermal and isothermal cavity, is shown to exist for any combination of the furnace-temperature profile and cavity-aperture diameter considered in this article (Sect. 5). The implications of this result for the practical application of deriving $\Delta T$ from the total reflectivity calculated for the isothermal cavity will be discussed.

Finally, in Sect. 6 we present results of measurements of the cavity radiance-temperature of two high-temperature fixed-point cells, enclosing an ingot of eutectic Re-C, of which the cavities are provided with different apertures. For $\lambda = 650\,\text{nm}$, the measured differences in cavity radiance-temperature are shown to be compatible with the differences in radiance temperature calculated for these cavities.

It should be stressed that uncertainties when quoted below are uncertainties in the modeled parameters emissivity and temperature drop, associated with the uncertainty in external conditions, such as the furnace-temperature profile. Uncertainties in the modeling, largely determined by the uncertainties in the thermophysical parameters involved, are not considered in this article.

Keeping track of the variation of the temperature drop $\Delta T$ and associated spectral and total emissivities when varying cell parameters (aperture diameter and temperature distribution) on the one hand and furnace-temperature profiles on the other hand, necessitates the introduction of an extensive range of quantities and symbols. A list of symbols utilized in this article is given above. Cell parameters are given in Sect. 2.

## 2 Experimental Context

Modeling has been performed for a cavity-crucible-furnace configuration, shown in Fig. 1, which in fact depicts an experimental setup presently in use at NMIJ. The Re-C eutectic cell is identified as 3S2, the furnace as VR10-A19 [5]. The furnace-temperature profile $T_{\text{f,low}}(x_{\text{f}})$ (full line, *Low profile*) given in Fig. 2 interpolates linearly between the temperatures of the front side of the radiation shields placed within the furnace tube in front of the Re-C fixed point (3S2) in study; $x_{\text{f}}$ is defined as the distance from the furnace center in the direction of the thermometer. The 'front-side temperatures' of the radiation shields are directly measured by means of the radiation

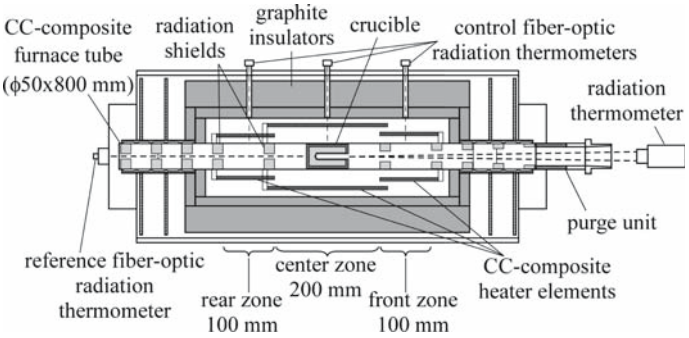


**Fig. 1** NMIJ three-zone furnace together with crucible, viewed by the thermometer through an assembly of radiation shields

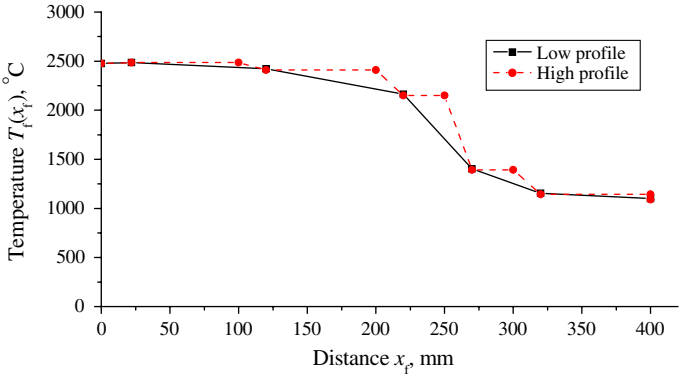


**Fig. 2** Measured and simulated furnace-temperature profiles $T_{f,low}(x_f)$ and $T_{f,high}(x_f)$. $x_f$ is the distance from the furnace center in the direction of the thermometer

thermometer (RT), LP-3 8040. The profile $T_{f,high}(x_f)$ (dashed line, *High profile*) has been constructed so as to represent the upper bound to the furnace-temperature profile from the point of view of the cavity: it assumes a uniform temperature of the tube sections between two neighboring radiation shields (front side and back side of a given shield are connected by the slanted dashed lines). The profiles $T_{f,low}(x_f)$ and $T_{f,high}(x_f)$ define the uncertainty band of the temperature profile from the point of view of the cavity.

The results presented below were calculated for the cylindro-conical cavity contained within the eutectic cell 3S2 assuming a diffusively reflecting grey cavity surface. Cavity dimensions: length $L = 45$ mm, diameter = 8 mm, tilt angle $\theta$ of the conical bottom 30°, without and with apertures, 3 mm or 5.5 mm in diameter; thickness of the cavity bottom: $d = 3$ mm. As in [2], in connection with the temperature drop for graphite we assumed $\varepsilon_g = 0.86$, thermal conductivity $K_g$ (at 2,750 K) = 36.4 $W \cdot m^{-1} \cdot K^{-1}$. Due to an oversight, cavity emissivities were calculated assuming $\varepsilon_g = 0.85$. This slight difference in graphite emissivity does not alter the conclusions of this article. The thermal conductivity of the Re-C eutectic ingot was taken as $K_{ingot}$ (at 2,750 K) = 55 $W \cdot m^{-1} \cdot K^{-1}$ [2].

## 3 Modeling Temperature Drop and Cavity Emissivity

### 3.1 Temperature Drop

The temperature drop $\Delta T$ is defined as $\Delta T = T_E - T_{cav}$, where $T_{cav}$ is taken as the areal average of the bottom temperature over the field of view (FOV) of the radiation thermometer LP-3 8040, 2.5 mm in diameter. All of the calculated results presented below, mostly taken from [2], are based upon simulations of the temperature drop $\Delta T$ at the end of the melting plateau in which—ideally—the liquid–solid interface coincides with the outer wall of the cavity tube. The simulations were performed using ANSYS, a finite-element software package; details are given in [2].

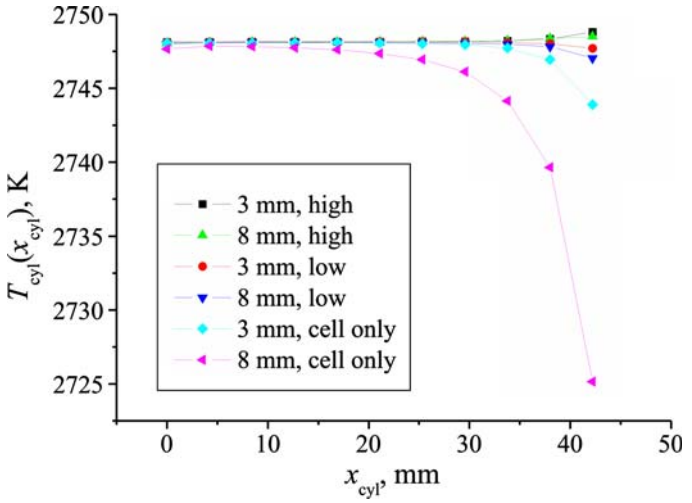


**Fig. 3** Cavity-temperature profiles along the main cylindrical section of the cavity, calculated for the cases $D = 8$ mm, cell only (triangles, left), $D = 3$ mm, cell only (diamonds), $D = 8$ mm, *low* (triangles, down), $D = 3$ mm, *low* (circles), $D = 8$ mm, *high* (triangles, up), $D = 3$ mm, *high* (squares). $x_{cyl}$ is the distance to the rim of the conical cavity bottom

### 3.2 Cavity Emissivity

Effective total and spectral emissivities—over the range 250 to 2,500 nm—were calculated using STEEP-3, a software package created by Prokhorov [6]. The emissivities, associated with a non-isothermal cavity, are defined as the areal averages of the local emittance averaged over the FOV of the radiation thermometer (2.5 mm in diameter), with $T_{cav}$ defined above as the reference temperature. The calculations were done (a) for the actual cavity-furnace configuration (Fig. 1), constituting the radiator, taking into account the temperature profile of the furnace tube within the limits *low* and *high*, i.e., $T_{f,low}(x_f)$, $T_{f,high}(x_f)$, (b) for an *isothermal* furnace-temperature profile $T_f(x_f) = T_{cav}$, and (c) for the *cell only*. The cavity geometry was specified in Sect. 2.

To evaluate the effect of the non-uniform temperature distribution within the cavity for the cases (a) and (c), calculations have been performed for (d) the *non-isothermal* cavity-temperature profiles, as calculated by means of ANSYS [1] and (e) for a hypothetical *isothermal* cavity-temperature profile $T = T_{cav}$ for cavity apertures $D$ of 3 mm, 5.5 mm, and 8 mm. It should be noted that the link (a)–(e) combines an *isothermal* cavity with a *non-uniform* furnace-temperature profile $T_{f,low}(x_f)$ or $T_{f,high}(x_f)$. Spectral and total emissivities for the cases (d), (e) are denoted as $\varepsilon(\lambda)$, $\varepsilon_{isoc}(\lambda)$ and $\varepsilon$, $\varepsilon_{isoc}$, respectively. For a given furnace-temperature profile $T_f(x_f)$ and a given cavity aperture $D$, the emissivities $\varepsilon_{isoc}(\lambda)$ and $\varepsilon_{isoc}$ turn out to be immune to the cavity temperature within a band around $T_{cav}$ comprising at least the maximum temperature drop (about 1 K) encountered in this study. Figure 3 shows examples of cavity temperature profiles $T_{cyl}(x_{cyl})$ along the cavity cylinder, whereby $x_{cyl}$ is defined as the distance with respect to the rim of the conical bottom, for the cases mentioned in the caption.

Results to be discussed below will be represented in terms of *reflectivities* $\rho(\lambda) = 1 - \varepsilon(\lambda)$, $\rho_{\mathrm{isoc}}(\lambda) = 1 - \varepsilon_{\mathrm{isoc}}(\lambda)$, and $\rho = 1 - \varepsilon$, $\rho_{\mathrm{isoc}} = 1 - \varepsilon_{\mathrm{isoc}}$ rather than in terms of their counterparts, i.e., the *emissivities* $\varepsilon(\lambda)$, $\varepsilon_{\mathrm{isoc}}(\lambda)$, and $\varepsilon$, $\varepsilon_{\mathrm{isoc}}$. Referring to reflectivity rather than to emissivity has the apparent advantage of a drastic reduction of significant digits to be specified. It should be mentioned in this respect that iteration precision is a critical aspect. Increasing the nominal precision in STEEP-3 from $10^{-6}$ to $10^{-8}$ sometimes produced a non-negligible systematic shift of the calculated result.

Finally, since the cavity cannot be treated as a separate unit, calculated reflectivities, to be discussed below, apply to the cavity-furnace combination as a whole, with the exception of the case 'cell only.'

## 4 Cavity Reflectivity: Influence of the Non-uniformity of the Cavity Temperature

### 4.1 Results

In Fig. 4, we show both $\rho_{\mathrm{isoc}}(\lambda)$ and $\rho(\lambda)$ as a function of $\lambda$, calculated within the range $\lambda = 250\,\mathrm{nm}$ to $\lambda = 2{,}500\,\mathrm{nm}$ for the profiles $T_{\mathrm{f,low}}(x_{\mathrm{f}})$ and $T_{\mathrm{f,high}}(x_{\mathrm{f}})$ (or, simply, *low* and *high*) and aperture diameters $D$ of 3 and 8 mm. The associated error $\Delta T_{\mathrm{isoc}}(\lambda) = T_{\mathrm{isoc}}(\lambda) - T_{\mathrm{cav}}$ is given in Fig. 5. Note that $\Delta T_{\mathrm{isoc}}(\lambda)$ is defined as the change in apparent cavity temperature at a given emission of the cavity (i.e., at a given signal, measured by the thermometer viewing the cavity) when replacing $\rho(\lambda)$ by $\rho_{\mathrm{isoc}}(\lambda)$.

It is of interest to compare the error $\Delta T_{\mathrm{isoc}}(\lambda)$ with the difference $T_{\mathrm{cav}}(\mathrm{high}) - T_{\mathrm{cav}}(\mathrm{low}) = \Delta T(\mathrm{low}) - \Delta T(\mathrm{high})$ associated with the difference between $T_{\mathrm{f,high}}(x_{\mathrm{f}})$

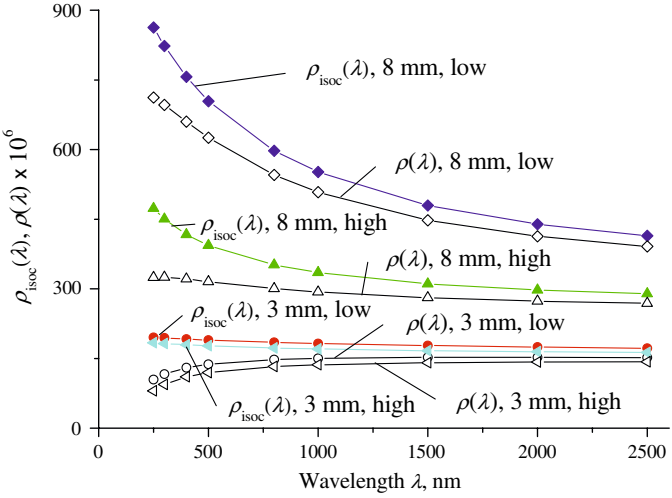


**Fig. 4** $\rho_{\mathrm{isoc}}(\lambda)$, $\rho(\lambda)$ versus $\lambda$ (Isothermal cavity/non-isothermal cavity): 8 mm-*low* (diamonds filled/diamonds open), 8 mm-*high* (triangles, up, filled/triangles, up, open), 3 mm-*low* (circles filled/circles open), 3 mm-*high* (triangles, left, filled/triangles, left, open)

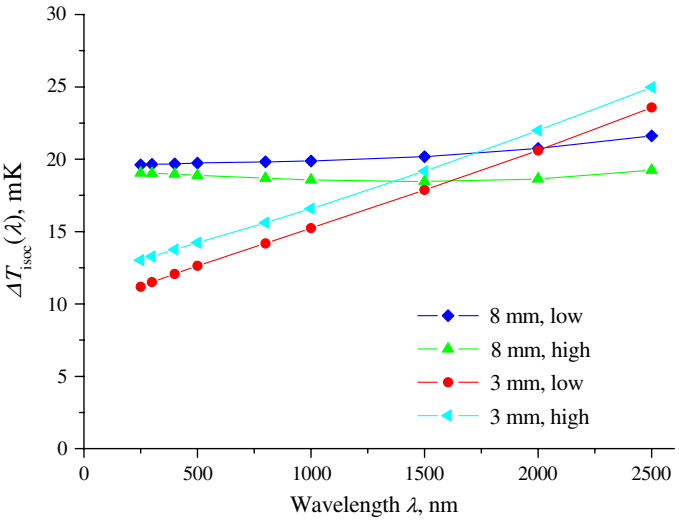


**Fig. 5** Effect $\Delta T_{\mathrm{isoc}}(\lambda)$ of the non-uniformity of the cavity temperature specified for different furnace-temperature profiles: 8 mm-*low* (diamonds), 8 mm-*high* (triangles, up), 3 mm-*low* (circles), 3 mm-*high* (triangles, left)

**Table 1** Compates $\Delta T_{\mathrm{isoc}}(\lambda)$ with $T_{\mathrm{cav}}(\mathrm{high}) - T_{\mathrm{cav}}(\mathrm{low})$. Specifies $\Delta T_{\mathrm{isoc}}$ (λ;cell)[a]

| $D$ mm | Furnace temperature profile | $\Delta T$ (mK) | $T_{\mathrm{cav}}(\mathrm{high}) - T_{\mathrm{cav}}(\mathrm{low})$ (mK) | $\Delta T_{\mathrm{isoc}}(\lambda)$ (mK) | $\Delta T_{\mathrm{isoc}}$ (λ;cell) (mK) |
|---|---|---|---|---|---|
| 3 | High | 82 | 10 | 15 | 20 |
| | Low | 92 | | 13 | 15 |
| 8 | High | 218 | 83 | 19 | 312 |
| | Low | 301 | | 20 | 218 |

[a] Reference wavelength of 650 nm

and $T_{\mathrm{f,low}}(x_{\mathrm{f}})$, the *high* and *low* furnace-temperature profile, respectively. This is done in Table 1, columns 4 and 5 with $\lambda = 650$ nm as the reference wavelength.

For the practically important case $D = 3$ mm, the error $\Delta T_{\mathrm{isoc}}(\lambda)$ is still larger than $T_{\mathrm{cav}}(\mathrm{high}) - T_{\mathrm{cav}}(\mathrm{low})$; the latter difference relates to the uncertainty in the cavity temperature $T_{\mathrm{cav}}$ due to the uncertainty in the furnace-temperature profile. Also indicated in Table 1 (last column) is $\Delta T_{\mathrm{isoc}}$ (λ; cell) $= T_{\mathrm{cav}}\{\rho_{\mathrm{av}}(\lambda)\} - T_{\mathrm{isoc}}$ (λ;cell), i.e., the error in the cavity temperature $T_{\mathrm{cav}}$ arising when replacing $\rho_{\mathrm{av}}(\lambda)$, averaged for the *high* and *low* furnace-temperature profiles, by $\rho_{\mathrm{isoc}}$ (λ;cell), calculated for the isothermal 'cell only,' again on the basis of the reference wavelength $\lambda = 650$ nm. The resulting deviations are noteworthy, since cavity emissivities for fixed-point radiators are currently calculated for a uniform cavity-temperature profile in conjunction with the case 'cell only.'

As follows from an inspection of Fig. 5, the errors $\Delta T_{\mathrm{isoc}}(\lambda)$ associated with differences in spectral emissivities calculated for the non-isothermal cavity and the isothermal cavity, although significant, do not depend strongly on the furnace-temperature

**Table 2** Demonstrating the insensitivity of $\Delta T_{\mathrm{isoc}}(\lambda)$ and $\Delta T_{\mathrm{isoc}}$ to the furnace-temperature profile

| Spectral reflectivity λ (nm) | $D$ (mm) | Furnace temperature profile | $\rho(\lambda) \times 10^6$ | $\rho_{\mathrm{isoc}}(\lambda) \times 10^6$ | $\Delta\rho(\lambda) \times 10^6$ | $\Delta T_{\mathrm{isoc}}(\lambda)$ (mK) | $\Delta\{\Delta T_{\mathrm{isoc}}(\lambda)\}$ (mK) |
|---|---|---|---|---|---|---|---|
| 650 | 8 | High | 313.7 | 368.8 | −55.1 | 18.8 | −1.0 |
| | | Low | 585.4 | 643.4 | −58.0 | 19.8 | |
| 950 | | High | 301.5 | 338.7 | −37.2 | 12.7 | −0.9 |
| | | Low | 521.9 | 561.7 | −39.8 | 13.6 | |
| 650 | 3 | High | 130.7 | 174.5 | −43.7 | 14.9 | 1.5 |
| | | Low | 147.7 | 187.0 | −39.4 | 13.4 | |
| 950 | | High | 170.8 | 138 | −32.8 | 11.2 | 1.0 |
| | | Low | 182.8 | 152.8 | −30.0 | 10.2 | |
| Total reflectivity | | | $\rho \times 10^6$ | $\rho_{\mathrm{isoc}} \times 10^6$ | $\Delta\rho \times 10^6$ | $\Delta T_{\mathrm{isoc}}$ (mK) | $\Delta(\Delta T_{\mathrm{isoc}})$ (mK) |
| | 8 | High | 287.9 | 310.3 | −22.4 | 15.4 | 2.6 |
| | | Low | 458.9 | 477.6 | −18.7 | 12.8 | |
| | 3 | High | 140.8 | 157.8 | −17.0 | 11.7 | 2.2 |
| | | Low | 153.3 | 167.2 | −13.9 | 9.5 | |

profile. This is more extensively assessed in Table 2 for apertures $D$ of 3 mm and 8 mm and for wavelengths of 650 and 950 nm. In this table, $\Delta\rho(\lambda) = \rho(\lambda) - \rho_{\mathrm{isoc}}(\lambda)$ and $\Delta\{\Delta T_{\mathrm{isoc}}(\lambda)\} = \Delta T_{\mathrm{isoc}}$ (λ;high) $-\Delta T_{\mathrm{isoc}}$ (λ;low), where $\Delta T_{\mathrm{isoc}}$ (λ;high) is associated with $T_{\mathrm{f,high}}(x_{\mathrm{f}})$ and $\Delta T_{\mathrm{isoc}}$ (λ;low) with $T_{\mathrm{f,low}}(x_{\mathrm{f}})$.

Also indicated in Table 2 are $\Delta\rho = \rho - \rho_{\mathrm{isoc}}$ and $\Delta(\Delta T_{\mathrm{isoc}}) = \Delta T_{\mathrm{isoc}}$ (high) $-\Delta T_{\mathrm{isoc}}$(low), where $\Delta T_{\mathrm{isoc}}$(high) is associated with $T_{\mathrm{f,high}}(x_{\mathrm{f}})$ and $\Delta T_{\mathrm{isoc}}$(low) with $T_{\mathrm{f,low}}(x_{\mathrm{f}})$. Again, we see that the errors $\Delta T_{\mathrm{isoc}}$ associated with differences in total emissivities calculated for the non-isothermal cavity and the isothermal cavity, although significant, do not depend strongly on the furnace-temperature profile.

Table 2 incorporates the sensitivity coefficient $\partial T_{\mathrm{cav}}/\partial\rho(\lambda) = \lambda T_{\mathrm{cav}}^2/c_2$, where $c_2$ is the second constant of Planck. For the case of practical importance $\lambda = 650$ nm, $D = 3$ mm, averaged for the high and low furnace-temperature profiles, it yields $\partial T_{\mathrm{cav}}/\partial\rho(\lambda) = 0.34 \times 10^6$ mK. This means that an uncertainty of 10 mK in $T_{\mathrm{cav}}$ would require an absolute uncertainty of $3 \times 10^{-5}$ in reflectivity $\rho(\lambda)$ or in emissivity $\varepsilon(\lambda)$ for a filter wavelength λ of 650 nm.

## 4.2 Discussion

### *4.2.1 Isothermal Cavity*

For the isothermal cavity, reflectivities $\rho_{\mathrm{isoc}}(\lambda)$ can be directly calculated by programs like STEEP-3 without the need for finite-element calculations to provide the non-isothermal cavity-temperature profiles, induced by the effects of the heat exchange within the cavity and between the cavity and furnace. The furnace-temperature profile needed to this end has to be measured anyhow in conjunction with the correction for the size-of-source effect. The configuration *isothermal cavity + furnace* just involves the

reflection of the furnace radiation, *external* to the cavity, by the cavity bottom, implying that the effective emissivity of the cavity-furnace combination is larger than that of the isothermal cavity only (cell only), or in terms of reflectivity $\rho_{\mathrm{isoc}}(\lambda) < \rho_{\mathrm{isoc}}\ (\lambda, \mathrm{cell})$.

### *4.2.2 Non-isothermal Cavity*

It should be noted (Fig. 4, Table 2) that the thermophysical processes involved tend to result in a *decrease* in the actual cavity reflectivities $\rho(\lambda)$—an increase in cavity emissivity $\varepsilon(\lambda)$—with respect to $\rho_{\mathrm{isoc}}(\lambda)$, subject to the constraint of uniformity in cavity temperature, $\rho(\lambda) < \rho_{\mathrm{isoc}}(\lambda)$, resulting in a positive value of the error $\Delta T_{\mathrm{isoc}}(\lambda)$, as indicated in Fig. 5. This can be understood as follows.

The change $\rho_{\mathrm{isoc}}(\lambda) \rightarrow \rho(\lambda)$ relates to the change in cavity-temperature profile from an isothermal profile with temperature $T_{\mathrm{cav}}$ all over the cavity to the actual non-isothermal profile. This is one of the consequences of the heat exchange (a) between the furnace and cavity and (b) within the cavity itself [2], entailing a heat-flow circuit: furnace tube → cavity wall → cavity bottom → ambient surrounding. This explains why for the actual non-isothermal cavity we invariably see $T_{\mathrm{cyl,B}} > T_{\mathrm{cav}} = T_{\mathrm{isoc}}$, in association with the heat-flow circuit, where $T_{\mathrm{cyl,B}}$ is the temperature of the cylindrical cavity surface near the cavity bottom of the non-isothermal cavity. This adds to the emission of the cavity via reflection, *internally*, of radiation from the nearby cylindrical cavity surface from the cavity bottom in the case of the non-isothermal cavity and thus to a higher overall emissivity $\varepsilon(\lambda)$ for the combination *non-isothermal cavity + furnace* as compared to $\varepsilon_{\mathrm{isoc}}(\lambda)$, enhanced just by the reflected *furnace* radiation, as explained in the paragraph above for the *isothermal cavity.*

Since $T_{\mathrm{cyl,B}} > T_{\mathrm{cav}}$, the spectrum of the radiation emitted by the nearby cylindrical cavity surface, and reflected by the cavity bottom, shows a shift toward lower wavelengths as compared to that emitted directly by the cavity bottom, which explains the increase of $\rho_{\mathrm{isoc}}(\lambda) - \rho(\lambda)$ with decreasing wavelength, shown in Fig. 4.

The insensitivity of $\Delta\rho(\lambda) = \rho(\lambda) - \rho_{\mathrm{isoc}}(\lambda)$ to the furnace-temperature profile—for a given cavity aperture—demonstrated in Fig. 4 and Table 2 has the prospect that, for a given cell, a reference reflectivity $\rho\{\lambda; T_{\mathrm{f,ref}}(x_{\mathrm{f}})\}$ would have to be calculated in full only once for a reference furnace-temperature profile $T_{\mathrm{f,ref}}(x_{\mathrm{f}})$ with say $T_{\mathrm{f,ref}}(x_{\mathrm{f}}) = \{T_{\mathrm{f,high}}(x_{\mathrm{f}}) + T_{\mathrm{f,low}}(x_{\mathrm{f}})\}/2$. For any other profile $T_{\mathrm{f}}(x_{\mathrm{f}})$, the associated reflectivity $\rho\{\lambda; T_{\mathrm{f}}(x_{\mathrm{f}})\}$ would follow, in principle, from $\rho\{\lambda; T_{\mathrm{f}}(x_{\mathrm{f}})\} = \rho_{\mathrm{isoc}}\{\lambda; T_{\mathrm{f}}(x_{\mathrm{f}})\} + \Delta\rho\{\lambda; T_{\mathrm{f,ref}}(x)\}$, where $\rho_{\mathrm{isoc}}\{\lambda; T_{\mathrm{f}}(x_{\mathrm{f}})\}$ is determined along with $T_{\mathrm{f}}(x_{\mathrm{f}})$, via STEEP -3, and $\Delta\rho\{\lambda; T_{\mathrm{f,ref}}(x_{\mathrm{f}})\} = \rho\{\lambda; T_{\mathrm{f,ref}}(x_{\mathrm{f}}))\} - \rho_{\mathrm{isoc}}\{\lambda; T_{\mathrm{f,ref}}(x_{\mathrm{f}})\}$ is supposed to be specified with the cell. The same would apply—*mutatis mutandis*—to the total reflectance $\rho$, cf. Table 2.

### *4.2.3 Optimizing the Cavity Geometry*

As shown in Table 1, the variation in cavity temperature $T_{\mathrm{cav}} = T_{\mathrm{E}} - \Delta T$ with furnace-temperature profile for $D = 8\,\mathrm{mm}$ is considerably larger than that for $D = 3\,\mathrm{mm}$. This is a strong argument for keeping the cavity reflectivity $\rho(\lambda)$ as close as possible to zero

**Table 3** Correlating the temperature drop $\Delta T$ with the total reflectivities $\rho_{\text{isoc}}$ and $\rho$

| $D$ (mm) | Furnace temperature profile | $\Delta T$ (mK) | $\rho_{\text{isoc}} \times 10^6$ | $\rho \times 10^6$ | $\Delta T_{\text{corr}}$ (mK) | $u(\Delta T_{\text{corr}})$ (mK) |
|---|---|---|---|---|---|---|
| 3 | Isothermal[a] | 71.7 | 142.0 | 128.1 | 0.6 | 2.1 |
| | High | 82.3 | 157.8 | 140.8 | 0.7 | 2.3 |
| | Low | 92.4 | 167.2 | 153.3 | 0.7 | 2.4 |
| | Cell only | 137.8 | 188.3 | 194.3 | 0.8 | 2.7 |
| 5.5 | Cell only | 449.6 | 603.3 | 616.1 | 2.6 | 8.7 |
| 8 | Isothermal[a] | 164.7 | 231.9 | 216.9 | 1.0 | 3.4 |
| | High | 217.6 | 310.3 | 287.9 | 1.4 | 4.5 |
| | Low | 301.1 | 477.6 | 458.9 | 2.1 | 6.9 |
| | Cell only | 846.8 | 1221.4 | 1199.3 | 5.3 | 17.7 |

[a] $T_{\text{f}}(x_{\text{f}}) = T_{\text{cav}}$

which—at least in the present cavity-furnace configuration—would imply keeping the diameter $D$ of the cavity aperture below about 3 mm.

It should be stressed that the prime parameter governing the contribution of the furnace to the overall reflectivity $\rho(\lambda)$ is the cavity reflectivity $\rho_{\text{isoc}}$ ($\lambda$;cell) rather than the cavity aperture $D$. The volume and shape of the cavity for a given $D$ could be further optimized—within the restrictions set by the furnace—so as to minimize $\rho_{\text{isoc}}$ ($\lambda$;cell) and thereby reduce the influence of the furnace. This would open opportunities for utilizing fixed-point radiators with relatively large cavity apertures, when fitted into the proper furnace.

## 5 Temperature Drop and its Relation with the Total Reflectivity

### 5.1 Results

The total reflectivity, although not of direct practical importance, may have an auxiliary function in estimating the temperature drop. As mentioned already in the introduction, the obvious issue here is to check for correlations between the temperature drop $\Delta T = T_{\text{E}} - T_{\text{cav}}$ and the total reflectivity $\rho$, noticing that both parameters are intimately connected with the total radiative flux emitted by the cavity. To this end, we have compiled in Table 3, columns 3–5, all the data obtained for the various cavity-furnace configurations considered and reviewed in Sect. 3.

The correlations between $\Delta T$ and $\rho_{\text{isoc}}$ on the one hand and $\Delta T$ and $\rho$ on the other hand, shown in Fig. 6, can be described by $\Delta T = A_{\text{isoc}} \cdot \rho_{\text{isoc}}$ and $\Delta T = A \cdot \rho$, with $A_{\text{isoc}} = 0.691 \times 10^{-6}$ mK, $u(A_{\text{isoc}}) = 0.015 \times 10^{-6}$ mK and $A = 0.705 \times 10^{-6}$ mK, $u(A) = 0.010 \times 10^{-6}$ mK. The quoted uncertainties are standard uncertainties.

### 5.2 Discussion

Of special interest is the correlation $\Delta T = A_{\text{isoc}} \cdot \rho_{\text{isoc}}$, since it would allow us to obtain the temperature drop $\Delta T$ from the total reflectivity $\rho_{\text{isoc}}$, bypassing the finite-element calculus, which would still be needed, however, at least for calculating the spectral reflectance $\rho\{\lambda; T_{\text{f,ref}}(x_{\text{f}})\}$ needed to determine the cavity temperature $T_{\text{cav}}$, as pointed out in the discussion to Sect. 4.2.

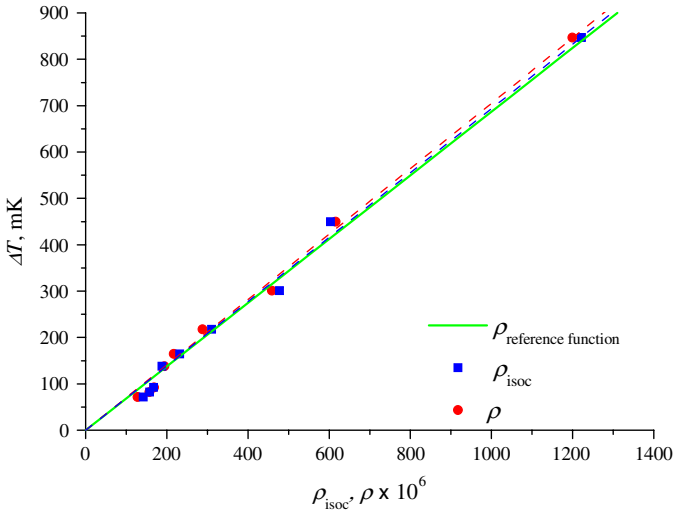


**Fig. 6** Temperature drop $\Delta T$ versus $\rho_{\mathrm{isoc}}$, $\rho$ for the cavity-furnace configurations defined in the first two columns of Table 3. Squares: $\rho_{\mathrm{isoc}}$, circles: $\rho$

The correlation in question will be considered in relation to the linear reference function $\Delta T = (T_{\mathrm{E}}/4) \cdot \rho \approx (T_{\mathrm{E}}/4) \cdot \rho_{\mathrm{isoc}}$, which is inferred from the following crude argument. We consider the fractional change $\Delta M/M$ in total radiance, or exitance, $M = \sigma \cdot T_{\mathrm{E}}^4$, exiting the aperture of the nearly closed cavity ($D \approx 0$), wall thickness $d$, with the outside of the cavity wall set to the temperature $T_{\mathrm{E}}$, when opening its window, i.e., its aperture with diameter $D > 0$. It invokes a fractional change $\Delta T/T_{\mathrm{E}}$ in the cavity temperature $T_{\mathrm{cav}}$ relative to $T_{\mathrm{E}}$, with $\Delta T = (T_{\mathrm{E}} - T_{\mathrm{cav}})$ given to first order by (a) $\Delta M/M = 4\Delta T/T_{\mathrm{E}}$. Formulating the change $\Delta M$ as $\Delta M = M - M'$, with $M' = \varepsilon\sigma T_{\mathrm{E}}^4$ leads to (b) $\Delta M/M = (1 - \varepsilon) = \rho$. Equating (a) and (b) yields the quoted reference function. Its slope $A_{\mathrm{ref}}$ (in mK) amounts to $A_{\mathrm{ref}} = 10^{-9} \cdot T_{\mathrm{E}}/4\,\mathrm{mK} = 0.687 \times 10^{-6}\,\mathrm{mK}$.

In column 6 of Table 3, we have specified the correction $\Delta T_{\mathrm{corr}} = [A_{\mathrm{isoc}} - A_{\mathrm{ref}}] \cdot \rho_{\mathrm{isoc}}$ to be applied relative to the reference function and in column 7, the uncertainty in the correction, $u(\Delta T_{\mathrm{corr}}) = u(A_{\mathrm{isoc}}) \cdot \rho_{\mathrm{isoc}}$, inferred from the scatter in the modeled data which is supposed to be related to scatter in the modeling errors. As may be appreciated from an inspection of the data, the corrections are only a fraction of the associated uncertainties, which gives some credit to the conjectured reference function. However, it remains to be seen whether or not the seemingly excellent agreement with the modeled isothermal-cavity data is only fortuitous. Some of the residuals $\Delta T(\mathrm{ANSYS}) - A_{\mathrm{isoc}} \cdot \rho_{\mathrm{isoc}}$ significantly exceed $u(\Delta T_{\mathrm{corr}})$; $\Delta T(\mathrm{ANSYS})$ refers to the temperature drop $\Delta T$, directly calculated by means of ANSYS. Further work is required to give a definitive assessment of the presented results. This should include redoing all the calculations for $\rho(\lambda)$ and $\rho_{\mathrm{isoc}}(\lambda)$ at a higher nominal precision (i.e., in STEEP-3 a precision of $10^{-8}$ rather than $10^{-6}$), especially for $D = 3\,\mathrm{mm}$. In addition, it should be investigated whether combining the influences of cavity aperture and furnace-temperature profile on $\Delta T$ as a lumped sum, as is done in the representation given in Fig. 6, is indeed a fruitful approach.

## 6 Temperature Drop: Model Versus Experiment

### 6.1 Introduction

$$\cos\theta \cdot \varepsilon_g \cdot \sigma \cdot T^4 \cdot \frac{d}{K_g} \cdot \left(\frac{r}{L}\right)^2 \tag{1}$$

For the freezing points of silver and gold, the following equation has been used to estimate the temperature drop $\Delta T$ across the back-wall of the cavity [7]:

$$\Delta T = \cos\theta \varepsilon_g \sigma T^4 \frac{d}{K_g} \left(\frac{r}{L}\right)^2 \tag{2}$$

where $\theta$ is the tilt angle of the conical bottom, $\varepsilon_g$ is the emissivity of graphite, $\sigma$ is the Stefan–Boltzmann constant, $T$ is the temperature in K, $d$ is the thickness of the cavity bottom, $K_g$ is the thermal conductivity of graphite, $r$ is the aperture radius, and $L$ is the cavity length. Numerical values are given in Sect. 2. As already shown in [2], this estimate can be considered an upper bound to $\Delta T$ since in its derivation the special effects of the heat exchange within the cavity (radiative and conductive) and between the cavity and furnace front end (radiative) have been disregarded.

### 6.2 Model

Table 4 shows the temperature drop $\Delta T$ (column 3) and the difference $T_{\mathrm{cav}} - T_\lambda$ between the true cavity temperature and associated radiance temperature (columns 4 and 5) for apertures of 3 and 8 mm, furnace-temperature profiles *high* and *low*, and wavelengths of 650 and 950 nm. As before, $\Delta T$ and $T_{\mathrm{cav}} = T_{\mathrm{E}} - \Delta T$ have been calculated by means of ANSYS, whereas $T_\lambda$ is derived from $T_{\mathrm{cav}}$ via the reflectivity $\rho(\lambda)$, derived by means of STEEP-3. As is seen, the shift in the radiance temperature $T_\lambda$ with respect to $T_{\mathrm{cav}}$ is significant, when compared with the temperature drop $\Delta T$. Finally, columns 6 and 7 show the differences $T_\lambda(3) - T_\lambda(8)$ in radiance temperatures pertinent to apertures of 3 mm and 8 mm, calculated for wavelengths of 650 nm and 950 nm, respectively.

In the table, third column, the results obtained for the temperature drop $\Delta T$ by means of ANSYS are compared with the corresponding ones derived from Eq. 2, which neglects the effects of heat exchange within the cavity and between the furnace and cavity—given in the last two rows. It is seen that Eq. 2 indeed constitutes an upper bound to $\Delta T$, as mentioned already in the introduction to this section.

### 6.3 Experiment

The experimental results given in the last two columns of Table 4 show the differences $T_\lambda(3) - T_\lambda(8)$ in radiance temperatures measured with LP-3 8040 for the cell 3S2 (a) without an aperture (8 mm) and (b) with a 3 mm aperture placed in front of the cavity tube, for filter wavelengths of 650 nm and 950 nm. The measurements were performed on two consecutive days. Drift of the radiation thermometer has been corrected by simultaneously measuring the radiance temperature of a second Re-C fixed point

**Table 4** Model: temperature drop $\Delta T$, difference $T_{cav} - T_\lambda$ between true cavity temperature and radiance temperature, difference $T_\lambda(3) - T_\lambda(8)$ between radiance temperatures pertinent to apertures of 3 mm and 8 mm

| Model | | | | | | | Experiment | |
|---|---|---|---|---|---|---|---|---|
| $D$ (mm) | Furnace temperature profile | $\Delta T$(mK) | $T_{cav} - T_\lambda$ | | $T_\lambda(3) - T_\lambda(8)$ | | $T_\lambda(3) - T_\lambda(8)$ | |
| | | | 650 nm (mK) | 950 nm (mK) | 650 nm (mK) | 950 nm (mK) | 650 nm (mK) | 950 nm (mK) |
| 3 | High | 82 | 45 | 69 | 198 | 216 | 140 ±80 | 130 ±30 |
| | Low | 92 | 50 | 76 | 358 | 392 | | |
| 8 | High | 218 | 107 | 150 | | | | |
| | Low | 301 | 200 | 259 | | | | |
| Eq. 2 | 3 mm | 219 | | | | | | |
| | 8 mm | 1,559 | | | | | | |

Experiment: difference $T_\lambda(3) - T_\lambda(8)$ between radiance temperatures measured for apertures of 3 mm and 8 mm

(1S1) on both days, realized in parallel in Nagano VR10-A20, a smaller variant of the VR10-A23 [5] furnace. The quoted standard uncertainties are based upon the repeatability of the melting temperatures, associated with the inflection points of the melting curves.

### 6.4 Discussion

As may be appreciated from an inspection of Table 4, for $\lambda = 650$ nm, modeled and experimental results obtained for $T_\lambda(3) - T_\lambda(8)$, shown in columns 6 and 8, respectively, agree within the standard uncertainty estimated for the experimental data, at least for the *high*-temperature profile, which indicates that this profile is closer to the profile actually seen by the cavity than the *low* profile. For $\lambda = 950$ nm, the result modeled for the high profile is closest to what was measured, but now the difference between modeled and measured results exceeds the estimated experimental standard uncertainty by about a factor of three.

## 7 Conclusions

From the above, it can be concluded that heat exchange between the cavity and furnace precludes treating the cavity as a separate unit; it has to be considered as an integral part of the cavity-furnace combination making up the fixed-point radiator in question.

The effect $\Delta T_{isoc}(\lambda)$ of the non-uniformity of the cavity temperature profile, induced by the heat exchange within the cavity and between the cavity and furnace cannot be neglected in view of the envisaged uncertainty of 50 mK in the realization of high-temperature fixed points. For apertures of 3 mm, $\Delta T_{isoc}(\lambda)$ turns out to be a considerable fraction of the temperature drop $\Delta T$.

The differences in emissivities calculated for the non-isothermal cavity and the isothermal cavity, although significant, do not depend strongly on the furnace-temperature profile, which might be of practical interest.

Uncertainties associated with the Monte–Carlo technique, utilized in calculating the effective emissivity of complex cavity-furnace configurations, should be quantitatively assessed. The sensitivity coefficient $\partial T_{\mathrm{cav}}/\partial\varepsilon(\lambda)$ increases quadratically with $T_{\mathrm{cav}}$: $\partial T_{\mathrm{cav}}/\partial\varepsilon(\lambda) = -\lambda T_{\mathrm{cav}}^2/c_2$. For the case considered, an uncertainty in the cavity temperature of 10 mK would require an uncertainty in the spectral emissivity (at 650 nm) of $3 \times 10^{-5}$.

The uncertainty in the dimensions defining the cavity-furnace configuration may have to be taken into account, since the *distribution* of the radiance in the front end of the furnace is expected to be a critical factor as well.

The uncertainty in the material parameters $K_g$ and $\varepsilon_g$ at high temperature may constitute a significant fraction of the overall uncertainty to be quoted for high-temperature fixed points. Therefore, finite-element modeling should be performed in which these parameters are varied to obtain the corresponding influence factors.

Results of such calculations may shed further light on the correlations between isothermal-cavity and non-isothermal-cavity reflectivity and between the temperature drop and total reflectivity. The sensitivity of the correlation factors in question to the cavity-furnace configuration is an issue here.

For reasons of practicality, blackbody simulators should be labelled by 'reflectivity' rather than by its complement, 'emissivity.'

**Acknowledgments** We are indebted to Dr. Alexander Prokhorov for consulting on the use of the software package STEEP-3. We wish to thank Dr. Naohiko Sasajima of NMIJ for the information on the furnace and its temperature distribution.

List of Symbols

| Symbol | Description |
|---|---|
| $T$ | Temperature (K) |
| $T_{\mathrm{FP}}$ | Fixed-point temperature |
| $T_{\mathrm{cav}}$ | Areal average of the cavity- bottom temperature over the field of view of the thermometer |
| $\Delta T$ | $T_{\mathrm{FP}} - T_{\mathrm{cav}}$ |
| $T_{\mathrm{E}}$ | Eutectic temperature of Re-C |
| $\lambda$ | Wavelength of observation |
| $T_\lambda$ | Radiance temperature at $\lambda$ |
| $T_\lambda(3)$ | Radiance temperature, measured for a cavity aperture of 3 mm |
| $T_\lambda(8)$ | Radiance temperature, measured for a cavity aperture of 8 mm |
| $x_{\mathrm{f}}$ | Distance from furnace center in the direction of the thermometer |
| $T_{\mathrm{f}}(x_{\mathrm{f}})$ | Furnace-temperature profile |
| $T_{\mathrm{f,low}}(x_{\mathrm{f}})$ | Lower bound to $T_{\mathrm{f}}(x_{\mathrm{f}})$ from the point of view of the cavity |
| $T_{\mathrm{f,high}}(x_{\mathrm{f}})$ | Upper bound to $T_{\mathrm{f}}(x_{\mathrm{f}})$ from the point of view of the cavity |

| | |
|---|---|
| $T_{\mathrm{cav}}(\mathrm{high})$ | $T_{\mathrm{cav}}$ corresponding to $T_{\mathrm{f,high}}(x_{\mathrm{f}})$ |
| $T_{\mathrm{cav}}(\mathrm{low})$ | $T_{\mathrm{cav}}$ corresponding to $T_{\mathrm{f,low}}(x_{\mathrm{f}})$ |
| $\Delta T(\mathrm{high})$ | $\Delta T$ corresponding to $T_{\mathrm{f,high}}(x_{\mathrm{f}})$ |
| $\Delta T(\mathrm{low})$ | $\Delta T$ corresponding to $T_{\mathrm{f,low}}(x_{\mathrm{f}})$ |
| $x_{\mathrm{cyl}}$ | Distance with respect to the rim of the conical bottom of the cavity along the cavity cylinder |
| $T_{\mathrm{cyl}}(x_{\mathrm{cyl}})$ | Cavity-temperature profile |
| $T_{\mathrm{cyl,B}}$ | $T_{\mathrm{cyl}}$ close to the cavity bottom: $T_{\mathrm{cyl,B}} > T_{\mathrm{cav}}$ due to the heat exchange between cavity and furnace |
| $T_{\mathrm{isoc}}(\lambda)$ | Apparent cavity temperature assuming the cavity temperature is uniform, derived from the associated spectral emissivity $\varepsilon_{\mathrm{isoc}}(\lambda)$, defined below. |
| $\Delta T_{\mathrm{isoc}}(\lambda)$ | $T_{\mathrm{isoc}}(\lambda) - T_{\mathrm{cav}}$ |
| $\Delta T_{\mathrm{isoc}}$ $(\lambda;\mathrm{high})$ | $\Delta T_{\mathrm{isoc}}(\lambda)$ associated with $T_{\mathrm{f,high}}(x_{\mathrm{f}})$ |
| $\Delta T_{\mathrm{isoc}}$ $(\lambda;\mathrm{low})$ | $\Delta T_{\mathrm{isoc}}(\lambda)$ associated with $T_{\mathrm{f,low}}(x_{\mathrm{f}})$ |
| $\Delta\{\Delta T_{\mathrm{isoc}}(\lambda)\}$ | $\Delta T_{\mathrm{isoc}}$ $(\lambda;\mathrm{high}) - \Delta T_{\mathrm{isoc}}$ $(\lambda;\mathrm{low})$ |
| $T_{\mathrm{isoc}}$ | Apparent cavity temperature assuming that the cavity temperature is uniform, derived from the associated total emissivity $\varepsilon_{\mathrm{isoc}}$, defined below. |
| $\Delta T_{\mathrm{isoc}}$ | $T_{\mathrm{isoc}} - T_{\mathrm{cav}}$ |
| $\Delta T_{\mathrm{isoc}}(\mathrm{high})$ | $\Delta T_{\mathrm{isoc}}$ associated with $T_{\mathrm{f,high}}(x_{\mathrm{f}})$ |
| $\Delta T_{\mathrm{isoc}}(\mathrm{low})$ | $\Delta T_{\mathrm{isoc}}$ associated with $T_{\mathrm{f,low}}(x_{\mathrm{f}})$ |
| $\Delta\{\Delta T_{\mathrm{isoc}}\}$ | $\Delta T_{\mathrm{isoc}}(\mathrm{high}) - \Delta T_{\mathrm{isoc}}(\mathrm{low})$ |
| $\varepsilon(\lambda)$ | Spectral emissivity cav+furn: areal average of the local spectral emittance averaged over the FOV of the thermometer, with $T_{\mathrm{cav}}$ as the reference temperature. |
| $\rho(\lambda)$ | Spectral reflectivity: $\rho(\lambda) = 1 - \varepsilon(\lambda)$ |
| $\varepsilon$ | Total emissivity cav+furn: areal average of the local total emittance averaged over the FOV of the thermometer, with $T_{\mathrm{cav}}$ as the reference temperature. |
| $\rho$ | Total reflectivity: $\rho = 1 - \varepsilon$ |
| $\varepsilon_{\mathrm{isoc}}(\lambda)$ | $\varepsilon(\lambda)$ calculated for cav+furn, assuming that the cavity temperature to be uniform at the temperature $T_{\mathrm{cav}}$,defined above |
| $\rho_{\mathrm{isoc}}(\lambda)$ | $1 - \varepsilon_{\mathrm{isoc}}(\lambda)$ |
| $\varepsilon_{\mathrm{isoc}}$ | $\varepsilon$ calculated for cav+furn, assuming the cavity temperature to be uniform at the temperature $T_{\mathrm{cav}}$, defined above |
| $\rho_{\mathrm{isoc}}$ | $1 - \varepsilon_{\mathrm{isoc}}$ |
| $\Delta\rho(\lambda)$ | $\rho(\lambda) - \rho_{\mathrm{isoc}}(\lambda)$ |
| $\Delta\rho$ | $\rho - \rho_{\mathrm{isoc}}$ |
| $\rho\{\lambda;\, T_{\mathrm{f}}(x_{\mathrm{f}})\}$ | $\rho(\lambda)$ corresponding to $T_{\mathrm{f}}(x_{\mathrm{f}})$, defined above |
| $\rho_{\mathrm{isoc}}\{\lambda;\, T_{\mathrm{f}}(x_{\mathrm{f}})\}$ | $\rho_{\mathrm{isoc}}(\lambda)$ corresponding to $T_{\mathrm{f}}(x_{\mathrm{f}})$ |
| $\rho\{\lambda;\, T_{\mathrm{f,high}}(x_{\mathrm{f}})\}$ | $\rho(\lambda)$ corresponding to $T_{\mathrm{f,high}}(x_{\mathrm{f}})$, defined above |
| $\rho\{\lambda;\, T_{\mathrm{f,low}}(x_{\mathrm{f}})\}$ | $\rho(\lambda)$ corresponding to $T_{\mathrm{f,low}}(x_{\mathrm{f}})$, defined above |
| $\rho_{\mathrm{av}}(\lambda)$ | $[\rho\{\lambda;\, T_{\mathrm{f,high}}(x_{\mathrm{f}})\} + \rho\{\lambda;\, T_{\mathrm{f,low}}(x_{\mathrm{f}})\}]/2$ |
| $T_{\mathrm{cav}}\{\rho_{\mathrm{av}}(\lambda)\}$ | $T_{\mathrm{cav}}$, calculated for $\rho_{\mathrm{av}}(\lambda)$ |

| | |
|---|---|
| $\rho_{\mathrm{isoc}}$ (λ;cell) | $\rho_{\mathrm{isoc}}(\lambda)$, calculated for the cell only, assuming that the cavity temperature is uniform |
| $T_{\mathrm{isoc}}$ (λ;cell) | Apparent cavity temperature, cell only, derived for the associated reflectivity $\rho_{\mathrm{isoc}}$ (λ;cell) |
| $\Delta T_{\mathrm{isoc}}$ (λ;cell) | $T_{\mathrm{cav}}\{\rho_{\mathrm{av}}(\lambda)\} - T_{\mathrm{isoc}}$ (λ;cell) |
| $T_{\mathrm{f,ref}}(x_{\mathrm{f}})$ | $\{T_{\mathrm{f,high}}(x_{\mathrm{f}}) + T_{\mathrm{f,low}}(x_{\mathrm{f}})\}/2$ |
| $\rho\{\lambda;\, T_{\mathrm{f,ref}}(x_{\mathrm{f}})\}$ | $\rho(\lambda)$corresponding to $T_{\mathrm{f,ref}}(x_{\mathrm{f}})$ |
| $\rho_{\mathrm{isoc}}\{\lambda;\, T_{\mathrm{f,ref}}(x_{\mathrm{f}})\}$ | $\rho_{\mathrm{isoc}}(\lambda)$ corresponding to $T_{\mathrm{f,ref}}(x_{\mathrm{f}})$ |
| $\Delta\rho\{\lambda;\, T_{\mathrm{f,ref}}(x_{\mathrm{f}})\}$ | $\rho\{\lambda;\, T_{\mathrm{f,ref}}(x_{\mathrm{f}})\} - \rho_{\mathrm{isoc}}\{\lambda;\, T_{\mathrm{f,ref}}(x_{\mathrm{f}})\}$ |
| $M$ | Exitance |
| $\sigma$ | Stefan-Boltzmann constant |
| $c_2$ | Second constant of Planck |
| $A$ | Defined via $\Delta T = A \cdot \rho$ |
| $A_{\mathrm{isoc}}$ | Defined via $\Delta T = A_{\mathrm{isoc}} \cdot \rho_{\mathrm{isoc}}$ |
| $A_{\mathrm{ref}}$ | $10^{-9} T_{\mathrm{E}}/4$ (mK) |
| $\Delta T_{\mathrm{corr}}$ | $[A_{\mathrm{isoc}} - A_{\mathrm{ref}}] \cdot \rho_{\mathrm{isoc}}$ |

## References


1. E.R. Woolliams, G. Machin, D. Lowe, R. Winkler, Metrologia **43**, R11 (2006)
2. P. Jimeno-Largo, Y. Yamada, P. Bloembergen, M.A. Villamanan, G. Machin, in Proceedings of TEMPMEKO 2004, 9th International Symposium on Temperature and Thermal Measurements in Industry and Science, ed. by D. Zvizdić, L. G. Bermanec, T. Veliki, T. Stašić (FSB/LPM, Zagreb, Croatia, 2004), pp. 335–340
3. P. Bloembergen, Y. Yamada, B.B. Khlevnoy, P. Jimeno-Largo, in *Proceedings of the 9th International Conference on New Developments and Applications in Optical Radiometry*, Davos, Switzerland, ed. by J. Groebner (Weltstrahlungszentrum, Davos, Switzerkland, 2005), pp. 283–284
4. P. Bloembergen, Y. Yamada, P. Jimeno-Largo, B.B. Khlevnoy, *ibid.*, pp. 287–288.
5. Y. Yamada, N. Sasajima, H. Gomi, T. Sugai, in *Temperature: Its Measurement and Control in Science and Industry*, Vol. 7, ed. by D. C. Ripple (AIP, New York, 2003), pp. 985–990
6. A.V. Prokhorov, Metrologia, **35**, 465 (1998)
7. J. Fischer, H.J. Jung, Metrologia **26**, 245 (1989)